

Recent b -Physics Results from CDF

Stephen P. Pappas
Yale University

The CDF Collaboration

As part of a broad program in b -physics, CDF has recently completed new measurements of the b -quark fragmentation fractions, performed a search for the rare decays $B^+ \rightarrow K^+ \mu^+ \mu^-$ and $B^0 \rightarrow K^* \mu^+ \mu^-$, and measured the polarization in the decays $B \rightarrow VV$. Previously reported fragmentation fractions are dominated by LEP results; CDF now adds measurements $f_u \equiv f_d = 37.1\% \pm 2.4\%$, $f_s = 16.6\% \pm 4.6\%$, $f_{\text{Baryon}} = 9.1\% \pm 3.0\%$ in an analysis of semi-leptonic decays, and the ratio $f_s/(f_u + f_d) = 20.1\% \pm 3.5\%_{-3.3\%}^{+3.9\%}$ in an independent analysis of sequential semileptonic decays. CDF's rare decay limits, $\mathcal{B}(B^+ \rightarrow K^+ \mu^+ \mu^-) < 5.2 \times 10^{-6}$ and $\mathcal{B}(B^0 \rightarrow K^{*0} \mu^+ \mu^-) < 4.0 \times 10^{-6}$ at 90% confidence level, are the most stringent to date. Finally, the polarization analysis for the decay modes $B \rightarrow J/\psi K^*$ and $B_s \rightarrow J/\psi \phi$ provides highly competitive results for the former mode and the first “full” analysis of the latter mode:

$$B_d : \begin{cases} A_0 = 0.770 \pm 0.039 \pm 0.012 \\ A_{\parallel} = (0.530 \pm 0.106 \pm 0.034)e^{(2.16 \pm 0.46 \pm 0.10)i} \\ A_{\perp} = (0.355 \pm 0.156 \pm 0.039)e^{(-0.56 \pm 0.53 \pm 0.12)i} \end{cases}$$
$$B_s : \begin{cases} A_0 = 0.778 \pm 0.090 \pm 0.012 \\ A_{\parallel} = (0.407 \pm 0.232 \pm 0.034)e^{(1.12 \pm 1.29 \pm 0.11)i} \\ |A_{\perp}| = 0.478 \pm 0.202 \pm 0.040 \end{cases}$$

I. INTRODUCTION

Without a doubt the most exciting prospect in b -physics in the near future is the observation of CP violation. However, this is clearly not all that is of interest in b -physics. The Tevatron's large b production cross section provides good opportunities to study a broad range of topics in b physics. We present the results of three recent analyses from CDF.

The first analysis measures b -hadron fragmentation fractions. Two methods are applied, the first of which identifies b -hadrons via their semileptonic decays to charmed hadrons. The charmed species are fully reconstructed and counted to derive the fragmentation fractions. The second method identifies B mesons from the sequential semileptonic decay of the b -quark followed by that of by the resulting c -quark. From this second method only the ratio of strange to light B mesons is determined.

The second analysis is a search for the rare decay modes $B^+ \rightarrow K^+ \mu^+ \mu^-$ and $B^0 \rightarrow K^{*0} \mu^+ \mu^-$. They are highly suppressed, being forbidden at tree level. This makes them a natural place to search for physics beyond the Standard Model. Observation of rates above the Standard Model prediction would indicate new physics. Current experiments are approaching these levels of sensitivity.

Finally, the polarization of vector-vector decays of B_d and B_s mesons provides information on decay dynamics of heavy-quark bound states and provides information relating to the possible use of these decays to study CP violation. In the best case the $J/\psi K^{*0}$ state is a P eigenstate and the decay $K^{*0} \rightarrow K_S \pi^0$ can be used for CP studies as simply as the gold-plated mode $B_d^0 \rightarrow J/\psi K_S$. If not, the decay angular distribution must be used to determine the CP content of the decay, but significant information can still be extracted.

II. B -QUARK FRAGMENTATION FRACTIONS

At the Tevatron b -quarks are produced as $b\bar{b}$ pairs in parton hard scattering. Since the hadrons escaping the primary interaction must be color singlets, additional quarks must become associated with the b -quarks in hadronization. This yields a long lived hadron containing a b -quark and a number of fragmentation particles. The quark(s) associated with the b determine the species of b -hadron observed, and the fragmentation fractions are defined as the relative fractions of the weakly decaying (*i.e.* long lived) b -hadrons:

$$f_{u,d,s,\text{Baryons}} = \frac{N(B_{u,d,s}, \Lambda_b)}{N(\text{all } b\text{-hadrons})} \quad (1)$$

Though the B_c meson has been observed [1], its production fraction is sufficiently small that we neglect it here. We similarly neglect b -baryons with additional heavy quarks as these are expected to be produced in very small quantities.

This analysis provides information on the processes of production and hadronization. Current results are dominated by LEP analyses [2] and hence come from an entirely different environment, potentially involving different QCD effects. A measurement at the Tevatron provides needed additional information on the hadronization process.

A. Semileptonic Analysis

Two approaches are taken to measuring the fragmentation fractions. The first is to look for b -hadrons via decay to an electron and a charmed hadron: $X_b \rightarrow e^+ \nu_e Y_c$. Decays to electrons are used because they have large acceptance in the trigger. We reconstruct the charmed state (D or Λ_c) via the following inclusive decay modes:

$$\begin{aligned} B^0 &\rightarrow e^+ \nu \ D^- X & B^0 &\rightarrow e^+ \nu \ D^{*-} X & B^+ &\rightarrow e^+ \nu \ \bar{D}^0 X \\ &\hookrightarrow K^+ \pi^- \pi^- & &\hookrightarrow \bar{D}^0 \pi^- & &\hookrightarrow K^+ \pi^- \\ & & &\hookrightarrow K^+ \pi^- & & \\ B_s^0 &\rightarrow e^+ \nu \ D_s^- X & \Lambda_b^0 &\rightarrow e^+ \nu \ \Lambda_c^- X \\ &\hookrightarrow \phi \pi^- & &\hookrightarrow \bar{p} K^+ \pi^- \\ &\hookrightarrow K^+ K^- & & \end{aligned} \quad (2)$$

The charmed hadrons are reconstructed from charged particle tracks found, assuming an appropriate mass. Since CDF does not have particle ID for individual particles, combinatoric backgrounds are large. The yields for the five above modes are given in Tab. I, and plots of the reconstructed peaks are shown in Fig. 1.

The event yields for the different decay chains are corrected for branching fractions and detector acceptance to yield the number of b -hadron candidates of each species. However, this process is complicated by cross talk from one channel to another and feed down from higher lying states. Monte Carlo simulation of the decay chains allows these effects to be measured. This yields a correction matrix from which b -hadron yields are calculated. Only ratios are calculated so that detector efficiencies and acceptances largely cancel. The residual differences are corrected for by the Monte Carlo calculation.

With the corrections in place, we can extract the following ratios of b -quark fragmentation fractions:

$$f_s/(f_u + f_d) = 22.3\% \pm 4.8\% \pm 5.6\% \quad f_{\text{Baryon}}/(f_u + f_d) = 12.3\% \pm 2.9\% \pm 3.2\% \quad (3)$$

If we assume $f_u + f_d + f_s + f_{\text{Baryon}} = 1$, *i.e.* no other long lived b -hadron species contribute to the decays, we find:

$$f_u \equiv f_d = 37.1\% \pm 2.4\% \quad f_s = 16.6\% \pm 4.6\% \quad f_{\text{Baryon}} = 9.1\% \pm 3.0\% \quad (4)$$

TABLE I. Signatures tagging b -hadron species: yields of charmed hadrons associated with e^\pm (see Sec. II A)

Decay	Yield	Decay	Yield	Decay	Yield
$B_d^0 \rightarrow D^-$	1463 ± 117	$B_d^0 \rightarrow D^{*-}$	393 ± 32	$B_u^+ \rightarrow D^0$	2756 ± 83
$B_s^0 \rightarrow D_s^-$	95 ± 14	$\Lambda_b^0 \rightarrow \Lambda_c^-$	227 ± 50		

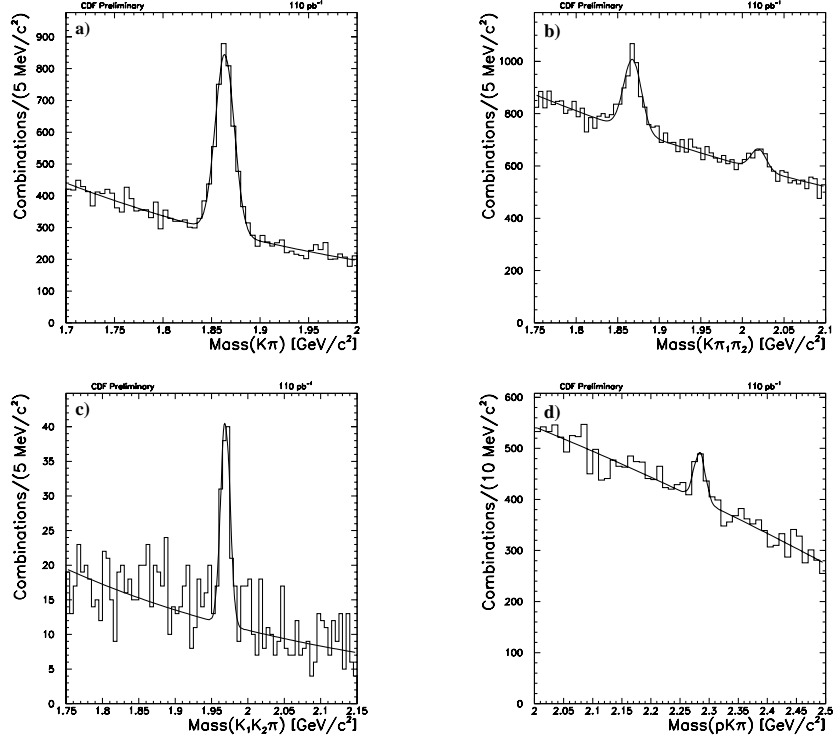


FIG. 1. Mass distributions of reconstructed charm species in association with an electron; as described in the text, these are our decay signatures for the decays: a) $B_u^+ \rightarrow \bar{D}^0$; b) $B_d^0 \rightarrow D^-, D^{*-}$; c) $B_s^0 \rightarrow D_s^-$; d) $\Lambda_b^0 \rightarrow \Lambda_c^-$

These should be compared with the current LEP averages [2]:

$$f_u \equiv f_d = 39.7\%_{-2.2\%}^{+1.8\%} \quad f_s = 10.5\%_{-1.7\%}^{+1.8\%} \quad f_{\text{Baryon}} = 10.1\%_{-3.1\%}^{+3.9\%} \quad (5)$$

B. Sequential Semileptonic Analysis

The second method determines b -quark fragmentation fractions from sequential semileptonic decays of $B_{u,d,s}$ mesons. The B meson decays semileptonically as does the resulting D meson. We choose dimuons to maximize the trigger acceptance; the trigger thresholds are lowest for this signature.

$$\begin{aligned}
B_d^0, B^+ &\rightarrow D^- \mu^+ \nu X & B_d^0, B^+ &\rightarrow \bar{D}^0 \mu^+ \nu X & B_s &\rightarrow D_s^- \mu^+ \nu X \\
&\hookrightarrow K^{*0} \mu^- \nu &&\hookrightarrow K^{*+} \mu^- \nu &&\hookrightarrow \phi \mu^- \nu \\
&\hookrightarrow K^+ \pi^- &&\hookrightarrow K_S^0 \pi^+ &&\hookrightarrow K^+ K^-
\end{aligned} \quad (6)$$

Finding a K^* or a ϕ associated with the muon pair tags the decay as being from a $B_{u,d}$ or a B_s meson. We seek K^* mesons reconstructed from $K\pi$ pairs ($K_S \rightarrow \pi^+ \pi^-$ for the K^{*+}), and ϕ mesons reconstructed from KK pairs. The B decay lepton is distinguished from the D decay lepton via its kinematics. It shows a charge correlation with the K for the neutral K^* decay and the charge of the K^* for the charged decay. This yields two interesting distributions: right and wrong sign charge correlation between the B muon and the K (K^*). The yields are shown in Tab. II and the reconstructed mass peaks in Fig. 2.

TABLE II. Signatures tagging B meson species: yields of K^* and ϕ mesons associated with $\mu^+ \mu^-$ pair (see Sec. II B)

Decay	Yield	Decay	Yield	Decay	Yield
$B_d^0, B_u^+ \rightarrow K^{*0}$	657 ± 55	$B_d^0, B_u^+ \rightarrow K^{*+}$	94 ± 21	$B_s^0 \rightarrow \phi$	103 ± 16

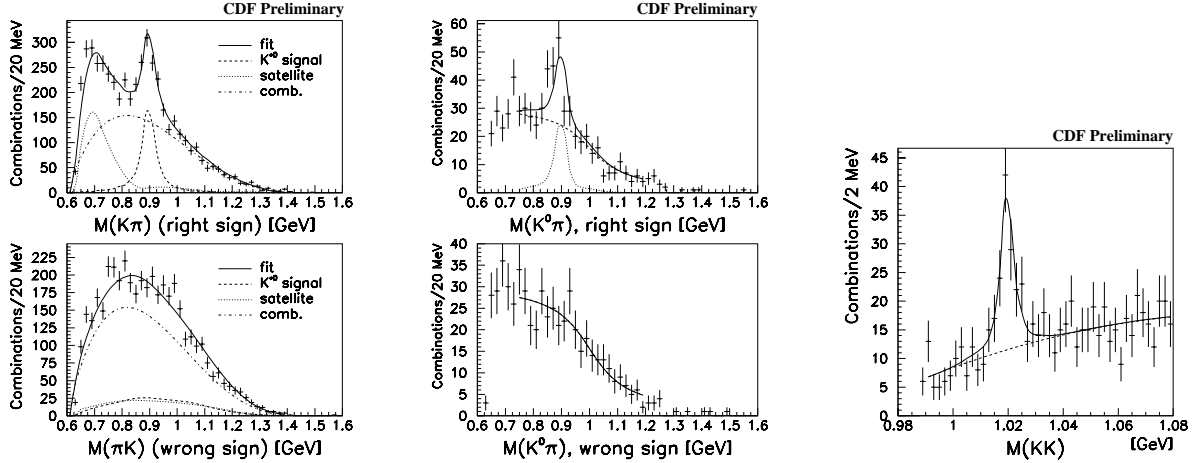


FIG. 2. Mass peaks of reconstructed K^* and ϕ mesons associated with an opposite sign dimuon pair. These signatures are used to tag the decaying B meson species as indicated in the text. The left and center plots are from reconstructing K^{*0} and K^{*+} produced by $B_{u,d}$ meson decays. The upper plot in each pair has the right sign charge correlation between the K (K^*) and the muon identified to be from the B decay. The right hand plot shows ϕ candidates indicating a B_s meson decay.

The so called “satellite” peak in the K^{*0} distributions (Fig. 2, left) results from processes like $B \rightarrow D^{*-} \mu^+ \nu X$, $D^{*-} \rightarrow \bar{D}^0 \pi^-$, $\bar{D}^0 \rightarrow K^+ \mu^- \nu$. This mimics the charge correlations and yields a mass peak from the kinematic correlation between the K and π . The shape of this satellite peak is determined from Monte Carlo simulation and added to the fits. With it included, the remaining (combinatoric) background matches between the right and wrong sign plots, allowing a more precise determination of the signal yield in the fit.

We correct for efficiency and acceptance differences between the modes, as well as cross talk and feed down, and correct for branching fractions into the observed modes. Taking account of the corrections, we obtain for the ratio of strange quark to light quark B meson fragmentation fractions:

$$f_s/(f_u + f_d) = (20.1 \pm 3.5^{+3.9}_{-3.3}) \quad (7)$$

This is in good agreement with the result of the first study.

III. RARE B DECAY SEARCH

The primary motivation to search for the rare decays $B^+ \rightarrow K^+ \mu^+ \mu^-$ and $B^0 \rightarrow K^* \mu^+ \mu^-$ is the potential to find physics beyond the Standard Model. Within the Standard Model, these decays occur only at the one or more loop level, making them strongly suppressed. New physics can markedly change the decay amplitudes by introducing new particles into the loop. Decays of B mesons are particularly interesting due to the large mass of the b -quark. Current data sets and search sensitivities are fast approaching some Standard Model predictions [3]. With luck, observation of some of the rare decays of B mesons is within reach.

We search for B meson candidates decaying to three and four tracks of which two are muons. We apply tight kinematic and quality cuts and calculate the dimuon and B candidate invariant masses. We observe resonant decays of the B mesons via the J/ψ and ψ' . Resonant (nonresonant) signal is defined as having a dimuon mass within (outside of) $200 \text{ MeV}/c^2$ of the nominal J/ψ mass or (and) within (outside of) $100 \text{ MeV}/c^2$ of the nominal ψ' mass. The invariant masses of candidate B mesons in resonant and nonresonant regions are shown in Fig. 3.

For the limits we assume all events in the search window are signal, and normalize the cross section to the resonant signal yield. The difference in detector acceptance due to different kinematics between resonant and nonresonant decays is determined from Monte Carlo simulation. We set 90% confidence level limits on the branching fractions:

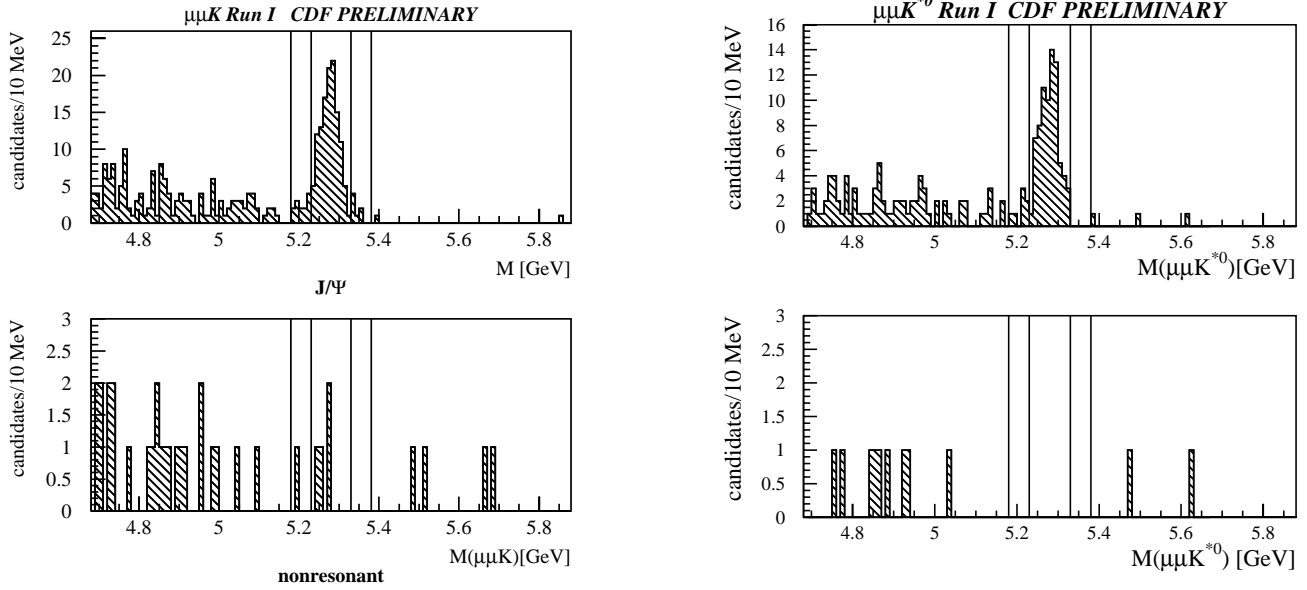


FIG. 3. Plots of invariant masses of B meson candidates for resonant (upper) and nonresonant (lower) dimuon invariant mass regions. The plots on the left are from the search for the rare decays of the B^+ meson, while the plots on the right are from the search for rare decays of the B^0 meson. The inner vertical lines represent the signal windows, while the outer lines and the plot boundaries indicate the sideband windows.

$$\mathcal{B}(B^+ \rightarrow K^+ \mu^+ \mu^-) < 5.2 \times 10^{-6} \quad \text{and} \quad \mathcal{B}(B^0 \rightarrow K^{*0} \mu^+ \mu^-) < 4.0 \times 10^{-6} \quad (8)$$

These results improve on the previous best limits (see [2]), and the result for $B^0 \rightarrow K^{*0} \mu^+ \mu^-$ approaches Standard Model predictions [3]:

$$\mathcal{B}(B^+ \rightarrow K^+ \mu^+ \mu^-) = 6.0 \times 10^{-7} \quad \text{and} \quad \mathcal{B}(B^0 \rightarrow K^{*0} \mu^+ \mu^-) = 2.9 \times 10^{-6} \quad (9)$$

If these predictions are accurate CDF should be able to see evidence of the K^{*0} decay in the 2fb^{-1} of data expected in Run 2.

IV. POLARIZATION IN $B \rightarrow V V$

The notation $B \rightarrow V V$ represents two decays: $B_d \rightarrow J/\psi K^*$ and $B_s \rightarrow J/\psi \phi$.

$$\begin{array}{l} B_d \rightarrow J/\psi K^* \\ \quad \hookrightarrow K^+ \pi^- \\ \quad \hookrightarrow \mu^+ \mu^- \end{array} \quad \begin{array}{l} B_s \rightarrow J/\psi \phi \\ \quad \hookrightarrow K^+ K^- \\ \quad \hookrightarrow \mu^+ \mu^- \end{array} \quad (10)$$

The polarizations of these decays provide tests of our understanding of the decay process and calculational methods. The B_d decay followed by $K^{*0} \rightarrow K_S \pi^0$ could also enhance statistical precision of CP violation studies versus using only the gold-plated mode $B^0 \rightarrow J/\psi K_S$ [4,5]. The $V V$ decays can have orbital angular momenta between the J/ψ and K^* (or ϕ) of 0, 1, or 2, so the parity of the system need not be well defined. This reduces the CP asymmetry observed. Previous results indicate the $V V$ states could be dominated by even orbital angular momentum, maximizing the observed CP asymmetry. A full angular analysis determines the parity-odd component of the decay amplitude.

Additional motivation comes from being able to measure the full angular decay distribution of the B_s decay. The angular information in this decay mode can enhance the sensitivity to a lifetime difference between the two mass eigenstates of the B_s [6]. This will become more interesting in Run 2.

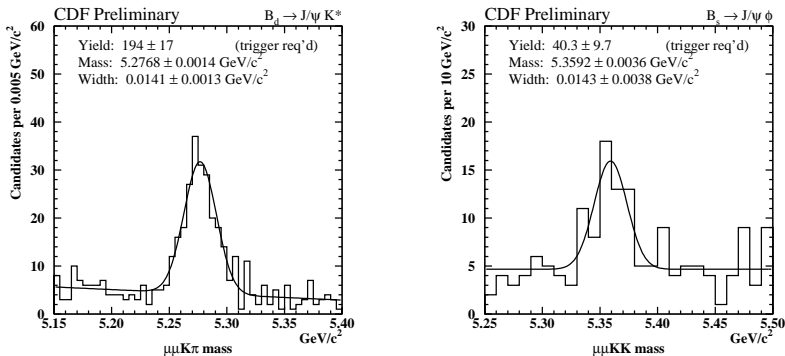


FIG. 4. Mass peaks from B_d (left) and B_s (right) candidates.

There are three matrix elements describing the transitions to the three eigenstates of the $J/\psi K^*$ system. This is usually described in the helicity basis, though a more interesting basis for us is the transversity basis [6–8]. In this formalism, the three matrix elements A_0 , A_{\parallel} , and A_{\perp} isolate states of definite parity, as well as isolating the longitudinal polarization state (A_0). The decay products of the vector mesons have three kinematic degrees of freedom, the decay angles, which we define according to the transversity formalism as in [7].

At tree level the decays proceed via internal W emission; this produces a c -quark and a $\bar{c}s$ quark pair in the final state together with the spectator from the B . For the J/ψ and the K^* (ϕ) to be color singlets the $\bar{c}s$ pair must be produced in the proper color state. Naively this occurs 1/3 of the time, but the remaining 2/3 of the time gluon exchange must occur to produce color singlets.

These decays are commonly calculated under the factorization ansatz, which treats the J/ψ as a current independent of the $B \rightarrow K^*$ current. One assumes the decay matrix elements factorize naturally into short and long distance (weak and strong) processes which do not interfere with each other. This predicts the matrix elements of the decay be relatively real. The observation of nontrivial matrix element phases implies final state interactions (though their absence does not rule out f.s.i.)

We reconstruct the decays by seeking first the J/ψ and then then adding other charged tracks for the hadrons. The decay angles and masses are calculated for fitting; the mass distributions of the B candidates are shown in Fig. 4.

Our candidate selection relies on the the long lifetime of the B mesons to suppress background. Reconstructed B meson candidates are required to have a long proper decay length compared with prompt background. We require a minimum reconstructed proper decay length of 100 μm for B_d candidates and 50 μm for B_s candidates. This can bias the angular distribution for the B_s since the mass eigenstates are approximately CP eigenstates and can have different lifetimes. The events determining matrix elements A_0 and A_{\parallel} are dominated by the approximately CP even mass eigenstate, while A_{\perp} is dominated by the approximately CP odd mass eigenstate. The matrix elements from the mass eigenstate with the longer lifetime can be enhanced.

The decay angular distribution is given by:

$$\begin{aligned}
\Omega_{\text{Trn}} \propto & 2 \cos^2 \Theta_{K^*} (1 - \sin^2 \Theta_T \cos^2 \Phi_T) |A_0|^2 + \sin^2 \Theta_{K^*} (1 - \sin^2 \Theta_T \sin^2 \Phi_T) |A_{\parallel}|^2 \\
& + \sin^2 \Theta_{K^*} \sin^2 \Theta_T |A_{\perp}|^2 + \frac{1}{\sqrt{2}} \sin 2\Theta_{K^*} \sin^2 \Theta_T \sin 2\Phi_T \text{Re}(A_0^* A_{\parallel}) \\
& \mp \sin^2 \Theta_{K^*} \sin 2\Theta_T \sin \Phi_T \text{Im}(A_{\parallel}^* A_{\perp}) \pm \frac{1}{\sqrt{2}} \sin 2\Theta_{K^*} \sin 2\Theta_T \cos \Phi_T \text{Im}(A_0^* A_{\perp})
\end{aligned} \tag{11}$$

The last two terms change sign for the decay of a \bar{B} as compared with a B . Whether a B_d or a \bar{B}_d decayed is known from the K charge, but the B_s and \bar{B}_s are not distinguishable by their final state particles. Hence, for B_s decays the last two terms cancel statistically and we lose all information about the phase of A_{\perp} .

We fit the angular distributions via a likelihood method, taking into account the detector acceptance and the background. Fig. 5 shows 68% confidence interval contours for the extracted decay matrix elements:

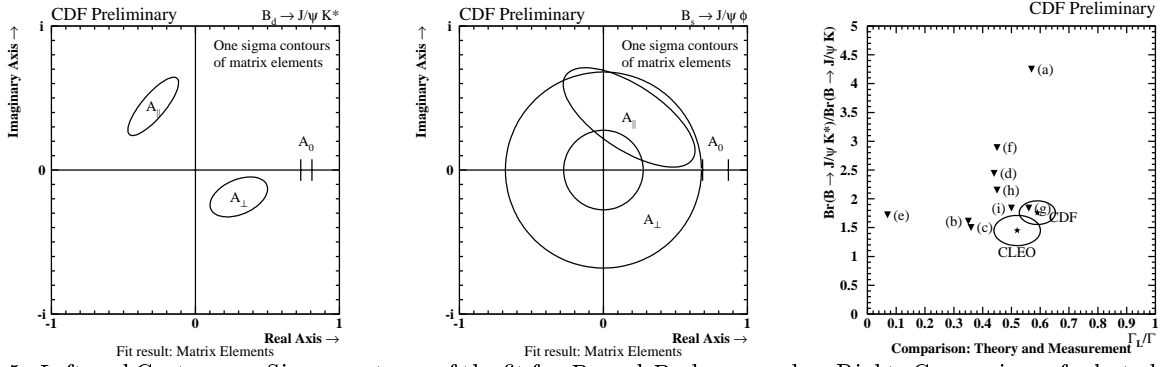


FIG. 5. Left and Center: one Sigma contours of the fit for B_d and B_s decay modes. Right: Comparison of selected predictions for B_d decay with current results; Ratio of branching ratios is plotted against longitudinal polarization fraction. (a) “BSW I”, (b) “BSW II”, (c) “CDDFGN”, (d) “JW” in [9]; (e) “ISGW”, (f) “IW(i)”, (g) “IW(ii)”, (h) “IW(iii)”, (i) “LF” in [10].

$$\begin{aligned}
 A_0 &= 0.770 \pm 0.039 \pm 0.012 & A_0 &= 0.778 \pm 0.090 \pm 0.012 \\
 A_{\parallel} &= (0.530 \pm 0.106 \pm 0.034)e^{(2.16 \pm 0.46 \pm 0.10)i} & \text{and} & A_{\parallel} &= (0.407 \pm 0.232 \pm 0.034)e^{(1.12 \pm 1.29 \pm 0.11)i} \\
 A_{\perp} &= (0.355 \pm 0.156 \pm 0.039)e^{(-0.56 \pm 0.53 \pm 0.12)i} & |A_{\perp}| &= 0.478 \pm 0.202 \pm 0.040
 \end{aligned} \quad (12)$$

A common test of theory is comparing measured results with both the predicted longitudinal polarization fraction ($\Gamma_{\perp}/\Gamma = |A_{\perp}|^2$) and the ratio of branching ratios $\mathcal{B}(B \rightarrow J/\psi K^*)/\mathcal{B}(B \rightarrow J/\psi K)$. Earlier results have shown a discrepancy; tuning predictions to improve one quantity worsened the other. Selected recent results of calculations are compared with measurements in Fig. 5 (right plot.) Predictions were selected from articles [9,10]. Agreement has improved, but the models still do not predict nontrivial matrix element phases. Our result implies some aspect of the physics is yet unaccounted for. Additional work by J. M. Soares was brought to the attention of the author at the conference; a summary can be found elsewhere in these proceedings.

Comparison of the B_d and B_s results indicates that $SU(3)_{\text{flavor}}$ is a valid approximation here, and that the B_s angular decay distribution contains significant information that could improve a lifetime difference measurement given larger data samples.

V. CONCLUSIONS AND OUTLOOK

All three of the analyses presented here have yielded significant b physics results from the Tevatron Run 1 data sample. They are among the most precise available and indicate very good prospects for Run 2 data sets. The rare decays could possibly lead to an observation with increased data samples, and the polarization will provide precision measurements of B decay parameters together with assisting in the measurement of lifetime differences in the B_s system.

-
- [1] F. Abe, *et al*, PRL **81** p. 2432 (1998)
 - [2] C. Caso *et al*, The European Physical Journal **C3** 1 (1998)
 - [3] A.Ali, C. Greub, T. Mannel, DESY Report, DESY 93-016 (1993)
 - [4] G. Valencia; Phys. Rev. D, **39**, 3339 (1989)
 - [5] G. Kramer, W. F. Palmer; Phys. Rev. D **45**, 193 (1992)
 - [6] A. Dighe, S. Sen; Phys. Rev. D **59** 074002 (1999)
 - [7] A. S. Dighe, I. Dunietz, H. J. Lipkin, J. L. Rosner; Phys. Lett. B **369** 144 (1996)
 - [8] A. S. Dighe, I. Dunietz, R. Fleischer; Fermilab preprint FERMILAB-PUB-98/093-T (*also hep-ph/9804253* 8 Apr 1998)
 - [9] M. Gourdin, A.N. Kamal, X. Y. Pham, PRL **73** p. 3355 (1994)
 - [10] H. Y. Cheng, Phys. Lett. B, p. 345 (1997); *also hep-ph/9610283* v2 19 Oct 1996